ELSEVIER

International Journal of Heat and Fluid Flow 20 (1999) 649–656

International Journal of HEAT AND FLUID FLOW

www.elsevier.com/locate/ijhff

The lateral movement of the three-dimensional cellular flame at low Lewis numbers

Satoshi Kadowaki

Department of Mechanical Engineering, Nagoya Institute of Technology, Gokiso-cho, Showa-ku, Nagoya 466-8555, Japan

Received 18 August 1998; accepted 26 February 1999

Abstract

The lateral movement of the three-dimensional (3-D) cellular flame at low Lewis numbers is numerically investigated. The equation used is the compressible Navier–Stokes equation including a one-step irreversible chemical reaction. We superimpose the hexagonal disturbance with the peculiar wave number on the stationary plane flame and calculate the evolution of the disturbed flame. When the Lewis number is unity, i.e., only the hydrodynamic effect has an influence on the flame instability, the stationary cellular flame is formed. When the Lewis number is lower than unity, i.e., the diffusive-thermal and hydrodynamic effects have an influence, the laterally moving cellular flame is formed. With a decrease in the Lewis number, the laterally moving velocity of the cell increases. The laterally moving velocity of the three-dimensional cellular flame is much larger than that of the two-dimensional (2-D) cellular flame. Because, the increment of local temperature at the convex flame front toward the unburned gas in the three-dimensional flame is great compared with that in the two-dimensional flame.

Keywords: Numerical simulation; Flame instability; Cellular flame

Notation

A_0	non-dimensional initial amplitude, referred to L
B	non-dimensional frequency factor, referred to U/L
D	diffusion coefficient
E	non-dimensional activation energy, referred to RT_0
e	non-dimensional stored energy, referred to $\rho_0 U^2$
L	characteristic length
Le	Lewis number ($=\alpha/D$)
$\mathrm{Le_c}$	critical Lewis number ($=1-2T_\mathrm{f}^2/E(T_\mathrm{f}-1)$)
Pe	Peclet number ($=UL/\alpha$)
Pr	Prandtl number ($=\nu/\alpha$)
p	non-dimensional pressure, referred to $\rho_0 U^2$
Q	non-dimensional heating value, referred to U^2
R	universal gas constant
S_u	non-dimensional burning velocity, referred to U
T	non-dimensional temperature, referred to T_0
T_0	temperature of the unburned gas
T_f	non-dimensional adiabatic flame temperature, referred to T_0
t	non-dimensional time, referred to L/U
U	characteristic velocity
V_L	non-dimensional laterally moving velocity of the cell, referred to U
u, v, w	non-dimensional velocities in x-, y-, and z-directions, referred to U
x, y, z	coordinates
Y	mass fraction of the unburned gas
Greek	
α	thermal diffusivity
γ	ratio of two specific heats
ΔL	non-dimensional moved distance of the cell, referred to L
δ	non-dimensional preheat zone thickness, referred to L
λ_y, λ_z	non-dimensional wavelengths in y- and z-directions, referred to L
λ_2	non-dimensional peculiar wavelength in the two dimensional flame, referred to L
ν	kinematic viscosity
ρ	non-dimensional density, referred to ρ_0
ρ_0	density of the unburned gas
ω	non-dimensional reaction rate, referred to $\rho_0 U/L$

1. Introduction

Premixed reactive gases do not always burn uniformly, and in many cases cellular flames appear. Cellular structures are formed owing mainly to the intrinsic instability of premixed flames. We know that the hydrodynamic effect caused by thermal expansion (Darrieus, 1938; Landau, 1944) and the diffusive-thermal effect caused by the preferential diffusion of mass versus heat (Barenblatt et al., 1962; Sivashinsky, 1977; Joulin and Mitani, 1981) are essential to intrinsic instability

E-mail address: kadowaki@megw.mech.nitech.ac.jp

0142-727X/99/$ - see front matter
PII: S0142-727X(99)00029-6

(Sivashinsky, 1983; Clavin, 1985; Williams, 1985; Law, 1988). In particular, the hydrodynamic effect is indispensable to the flame instability since all flames in gaseous mixtures are attended with thermal expansion.

The cellular flames exhibit temporal motion under certain conditions (Markstein, 1964; Sabathier et al., 1981; Gololobov et al., 1981; Gorman et al., 1994; Pearlman and Ronney, 1994). To study the temporal motion of the flame front, non-linear analysis was performed, based on the diffusive-thermal model, including the so-called Kuramoto–Sivashinsky (KS) equation, and on the Michelson–Sivashinsky (MS) equation (Michelson and Sivashinsky, 1982; Sivashinsky, 1983; Hyman and Nicolaenko, 1986; Denet and Haldenwang, 1992). It was shown that the temporal motion of cellular flames appears at low Lewis numbers. However, the results obtained in analyses based on the diffusive-thermal model are valid only for flames with small enough heat release since the hydrodynamic effect is disregarded in this model. The results obtained through the MS equation are valid for flames with small expansion coefficients since the constant-density approximation is used in the derivation of this equation. In addition, both the KS and MS equations are available for weakly non-linear analysis.

In general, premixed flames, e.g., hydrogen–air and methane–air flames with stoichiometric conditions, have considerably large heat release. Thus, the hydrodynamic effect caused by thermal expansion plays an important role in the instability of premixed flames. This means that the diffusive-thermal model is invalid for these flames. Therefore, we need to use the compressible Navier–Stokes (NS) equation, which is valid for large heat release, in the study of the temporal motion of premixed gaseous flames.

The numerical calculation based on the compressible NS equation was performed to study the instability of flame fronts, where the hydrodynamic effect was taken into account (Denet, 1993; Patnaik and Kailasanath, 1994; Denet and Haldenwang, 1995 Kadowaki, 1995; Bychkov et al., 1996). The unstable motion of flame fronts and the structure of cellular flames were investigated in detail, and it was reported that the hydrodynamic effect has a great influence on the flame instability. Thereafter, the lateral movement of cellular flames was numerically studied, in which the compressible NS equation was used (Kadowaki, 1997). It was shown that laterally moving cells appear not only at $\mathrm{Le} < \mathrm{Le_c}$ but also at $\mathrm{Le_c} < \mathrm{Le} < 1$, which is different from the results obtained in the calculations based on the diffusive-thermal model (Margolis and Matkowsky, 1983; Bayliss and Matkowsky, 1992; Daumont et al., 1997), and that the non-linear effect of the flame front and the Lewis number effect are essential factors in the appearance of the lateral movement of cells.

The numerical calculation on the lateral movement of cells dealt only with the two-dimensional flame (Kadowaki, 1997). However, the three-dimensional flame is usually observed under most experimental conditions since the two-dimensional flame requires a special experimental setup. In addition, we know the difference in structure between two- and three-dimensional cellular flames. For example, the disposition of cells and the spacing between cells in the three-dimensional flame are considerably different from those in the two-dimensional flame (Kadowaki, 1996). Thus, it is very important to study the lateral movement of the three-dimensional cellular flame and to compare with the results of the two-dimensional flame.

In the present study, we calculate the three-dimensional unsteady reactive flow to investigate the lateral movement of cellular flames at low Lewis numbers using the compressible NS equation. We obtain the laterally moving velocity of the cell and compare with that of the two-dimensional flame. Moreover, we study the mechanism of the appearance of the lateral movement of two- and three-dimensional cellular flames.

2. Governing equations

We consider the single-reactant flame, where the abundant component is excessive and the chemical reaction is controlled only by the deficient component. We calculate the three-dimensional unsteady reactive flow and take the direction tangential to the flame front as the yz-surface, with the gas velocity in the positive x-direction. In the derivation of the governing equations, the following assumptions are used: (1) Only two species, unburned and burned gases, are present. Both gases are ideal and have the same molecular weights and the same Lewis numbers. (2) The chemical reaction is an exothermic one-step irreversible reaction, and the reaction rate has the Arrhenius form. (3) The specific heats and transport coefficients are constant throughout the whole region. (4) The radiation, bulk viscosity, Soret effects, Dufour effects, and pressure gradient diffusion are negligible, and the viscous term in the energy equation is disregarded.

The flow variables in the governing equations are non-dimensionalized by the characteristic length, the characteristic velocity, and the density of the unburned gas. The characteristic length is 80 times the preheat zone thickness, where the latter is defined as the thermal diffusivity divided by the burning velocity. The characteristic velocity is the isothermal sound velocity of the unburned gas. The governing equations are written in the formation of the conservation law

$$\frac{\partial \mathbf{U}}{\partial t}+\frac{\partial \mathbf{F}}{\partial x}+\frac{\partial \mathbf{G}}{\partial y}+\frac{\partial \mathbf{H}}{\partial z}=\mathbf{S}, \tag{1}$$

where $\mathbf{U}$, $\mathbf{F}$, $\mathbf{G}$, $\mathbf{H}$, and $\mathbf{S}$ are vectors given by

$$\mathbf{U}=\begin{pmatrix}\rho\\ \rho u\\ \rho v\\ \rho w\\ e\\ \rho Y\end{pmatrix},$$

$$\mathbf{F}=\begin{pmatrix}\rho u\\ \rho u^2+p-\frac{\mathrm{Pr}}{\mathrm{Pe}}\left(\frac{4}{3}\frac{\partial u}{\partial x}-\frac{2}{3}\frac{\partial v}{\partial y}-\frac{2}{3}\frac{\partial w}{\partial z}\right)\\ \rho uv-\frac{\mathrm{Pr}}{\mathrm{Pe}}\left(\frac{\partial v}{\partial x}+\frac{\partial u}{\partial y}\right)\\ \rho uw-\frac{\mathrm{Pr}}{\mathrm{Pe}}\left(\frac{\partial w}{\partial x}+\frac{\partial u}{\partial z}\right)\\ (e+p)u-\frac{1}{\mathrm{Pe}}\frac{\gamma}{\gamma-1}\frac{\partial T}{\partial x}\\ \rho Yu-\frac{1}{\mathrm{Pe\,Le}}\frac{\partial Y}{\partial x}\end{pmatrix},$$

$$\mathbf{G}=\begin{pmatrix}\rho v\\ \rho uv-\frac{\mathrm{Pr}}{\mathrm{Pe}}\left(\frac{\partial v}{\partial x}+\frac{\partial u}{\partial y}\right)\\ \rho v^2+p-\frac{\mathrm{Pr}}{\mathrm{Pe}}\left(\frac{4}{3}\frac{\partial v}{\partial y}-\frac{2}{3}\frac{\partial u}{\partial x}-\frac{2}{3}\frac{\partial w}{\partial z}\right)\\ \rho vw-\frac{\mathrm{Pr}}{\mathrm{Pe}}\left(\frac{\partial w}{\partial y}+\frac{\partial v}{\partial z}\right)\\ (e+p)v-\frac{1}{\mathrm{Pe}}\frac{\gamma}{\gamma-1}\frac{\partial T}{\partial y}\\ \rho Yv-\frac{1}{\mathrm{Pe\,Le}}\frac{\partial Y}{\partial y}\end{pmatrix},$$

$$\mathbf{H}=\begin{pmatrix}\rho w\\ \rho uw-\frac{\mathrm{Pr}}{\mathrm{Pe}}\left(\frac{\partial w}{\partial x}+\frac{\partial u}{\partial z}\right)\\ \rho vw-\frac{\mathrm{Pr}}{\mathrm{Pe}}\left(\frac{\partial w}{\partial y}+\frac{\partial v}{\partial z}\right)\\ \rho w^2+p-\frac{\mathrm{Pr}}{\mathrm{Pe}}\left(\frac{4}{3}\frac{\partial w}{\partial z}-\frac{2}{3}\frac{\partial u}{\partial x}-\frac{2}{3}\frac{\partial v}{\partial y}\right)\\ (e+p)w-\frac{1}{\mathrm{Pe}}\frac{\gamma}{\gamma-1}\frac{\partial T}{\partial z}\\ \rho Yw-\frac{1}{\mathrm{Pe\,Le}}\frac{\partial Y}{\partial z}\end{pmatrix},$$

$$\mathbf{S} = \begin{pmatrix} 0 \\ 0 \\ 0 \\ 0 \\ QB\rho Y \exp(-E/T) \\ -B\rho Y \exp(-E/T) \end{pmatrix}.$$

The equation of state is

$$p = \rho T. \tag{2}$$

3. Numerical procedures

The physical parameters are given to simulate a gas mixture of which the burning velocity is 0.83 m/s and the adiabatic flame temperature is 2086 K at atmospheric pressure and room temperature. The non-dimensional burning velocity $S_u = 2.5 \times 10^{-3}$, and the non-dimensional adiabatic flame temperature $T_f = 7.0$. Non-dimensional parameters used are $\mathrm{Pe} = 3.2 \times 10^4$, $\mathrm{Pr} = 1.0$, $\gamma = 1.4$, $Q = 21$, and $E = 70$. For the study of the Lewis number effect, we take $\mathrm{Le} = 0.5$, 0.6, 0.7, 0.8, and 1.0, since we are interested only in the lateral movement of cellular flames at $\mathrm{Le} \leqslant 1$. The frequency factor is determined by the condition under which the flame velocity of a plane flame is equal to the set burning velocity ($= 2.5 \times 10^{-3}$). For the flames of $\mathrm{Le} = 0.5$, 0.6, 0.7, 0.8, and 1.0, we set $B = 2.17 \times 10^6$, 1.85×10^6, 1.62×10^6, 1.44×10^6, and 1.20×10^6, respectively.

Initial conditions are provided by the solution of the stationary plane flame (Fig. 1). On the flame we superimpose a hexagonal disturbance (Christopherson, 1940) since well-regulated hexagonal cells are experimentally observed in flames with broad enough surfaces (Searby and Quinard, 1990) and the hexagonal pattern of cells are shown analytically and numerically (Shtilman and Sivashinsky, 1990). The displacement of the flame front in the x-direction due to the disturbance is given by

$$\sin(2\pi y/\lambda_y)\sin(2\pi z/\lambda_z) - \cos(4\pi z/\lambda_z)/2, \tag{3}$$

where the relation $\lambda_z = \lambda_y\sqrt{3}$ is realized. The wavelength is set equal to the wavelength corresponding to the maximum growth rate, i.e., the peculiar wavelength, since the spacing between cells on the flame is equivalent to the peculiar wavelength. The peculiar wavelength is obtained from the dispersion relation, which is given by the calculation for sufficiently small disturbances. The peculiar wavelengths for $\mathrm{Le} = 0.5$, 0.6, 0.7, 0.8, and 1.0 in the three-dimensional flame are shown in Table 1, where the non-dimensional preheat zone thickness $\delta = 1/80 = 1.25 \times 10^{-2}$. In addition, the peculiar wavelengths in the two-dimensional flame are shown in Table 2, where λ_2 is $(1/2)\sqrt{3}$ times λ_y (Kadowaki, 1996). Since the peculiar wavelength is chosen in the present calculation, neither cell merging nor tip splitting is observed. This behavior of the flame front is obtained when shorter and longer wavelengths are chosen (Denet, 1993; Denet and Bonino, 1994).

Boundary conditions are as follows: In the x-direction, except for the velocity of inlet flow, free flow conditions are used upstream and downstream. The inlet-flow velocity is set to the burning velocity so that the flame position will barely move. In y- and z-directions, spatially periodic conditions are used, since broad enough flame surfaces are treated in the present study. Thus, the results on the temporal motion of fronts are valid for flames with broad enough surfaces.

The explicit MacCormack scheme (MacCormack and Baldwin, 1975), which has second-order accuracy in both time and space, is adopted for the calculation. The computational domain is double the characteristic length in the x-direction and one wavelength of the disturbance in y- and z-directions, which is resolved by a $261 \times 31 \times 53$ variably spaced grid for $\mathrm{Le} = 0.6$, 0.7, 0.8, and 1.0, and by a $261 \times 46 \times 79$ grid for $\mathrm{Le} = 0.5$. The minimum grid size in the x-direction is 2.5×10^{-3}. These grids are fine enough to prevent numerical errors from contaminating the solutions. The time-step interval is 5×10^{-4}. For one time step, required CPU times are 0.34 and 0.75 s for the $261 \times 31 \times 53$ and $261 \times 46 \times 79$ grids, respectively, on a FUJITSU VPP500 supercomputer. Each computation time ranges between 15 and 19 h.

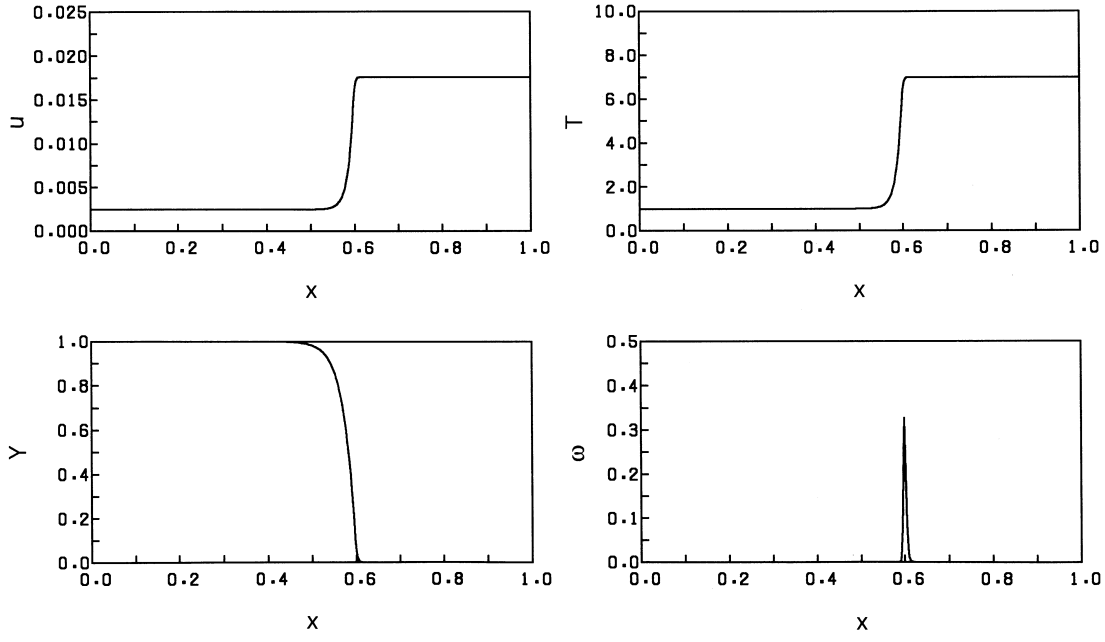

Fig. 1. Distributions of the velocity, the temperature, the mass fraction of the unburned gas, and the reaction rate in the stationary plane flame for $\mathrm{Le} = 0.5$.

Table 1
Peculiar wavelengths for Le = 0.5–1.0 in the three-dimensional flame

Le	λ_y	λ_z	λ_y/δ	λ_z/δ
0.5	0.166	0.288	13.3	23.0
0.6	0.185	0.320	14.8	25.6
0.7	0.207	0.358	16.6	28.6
0.8	0.251	0.436	20.1	34.9
1.0	0.494	0.855	39.5	68.4

Table 2
Peculiar wavelengths for Le = 0.5–1.0 in the two-dimensional flame

Le	λ_2	λ_2/δ
0.5	0.144	11.5
0.6	0.160	12.8
0.7	0.179	14.3
0.8	0.218	17.4
1.0	0.427	34.2

4. Results and discussion

First, we set Le = 0.5 to study the diffusive-thermal and hydrodynamic effects on the lateral movement of cellular flames. We superimpose the disturbance with $A_0 = 1 \times 10^{-2}$, $\lambda_y = 0.166$, $\lambda_z = 0.288$ on the plane flame and calculate the evolution of the disturbed flame front. The flame fronts at $t = 0$, 15, and 40 are illustrated in Fig. 2. The schematic domain is $3\lambda_y \times 2\lambda_z$. The location of the flame front is defined as the position where $T = 5.0$. The unburned gas flows in from the bottom at the burning velocity, and the burned gas flows out to the top. The disturbance grows initially with time, and its amplitude reaches the maximum. The flame front changes from a sinusoidal to a cellular shape ($t = 15$). Thereafter, the cellular flame moves upstream. This denotes that the flame velocity has increased, which is due to the increment of the flame-surface area and to the variation in local flame velocity.

To study the lateral movement of cells, we illustrate the distributions of cells in the yz-plane at $t = 0$, 15, and 40 in Fig. 3, where the schematic domain is $3\lambda_y \times 2\lambda_z$. We take notice of the cell which is written 'cell' in the figure. The spacing between hexagonal cells is equal to λ_y ($= 13.3\ \delta$), and it is longer than that of the two-dimensional flame ($= 11.5\delta$). After the formation of the cellular flame, the cell moves to the right-bottom. This indicates that the three-dimensional cellular flame moves laterally, just as the two-dimensional cellular flame did. To obtain the laterally moving velocity of the cell, we show the moved distance of the cell in the yz-plane in Fig. 4. From the gradient of the straight line, we find that the laterally moving velocity $V_L = 4.78 \times 10^{-3}$ ($= 1.91 S_u$). This value is much larger than that of the two-dimensional flame ($= 0.79 S_u$).

We next set Le = 0.6 and superimpose the disturbance with $A_0 = 1 \times 10^{-2}$, $\lambda_y = 0.185$, $\lambda_z = 0.320$. The distributions of cells at $t = 0$, 30, and 80 are illustrated in Fig. 5. The disturbance superimposed grows initially, and the cellular structure of the flame front appears at $t = 30$. After that, the cell moves to the right-bottom, same as the Le = 0.5 flame. The laterally moving velocity of the cell is 2.37×10^{-3} ($= 0.95 S_u$), which is smaller than that of the Le = 0.5 flame ($= 1.91 S_u$) and is larger than that of the two-dimensional flame for Le = 0.6 ($= 0.41 S_u$).

We make the Lewis number higher. We set Le = 0.8 and superimpose the disturbance with $A_0 = 1 \times 10^{-2}$, $\lambda_y = 0.251$,

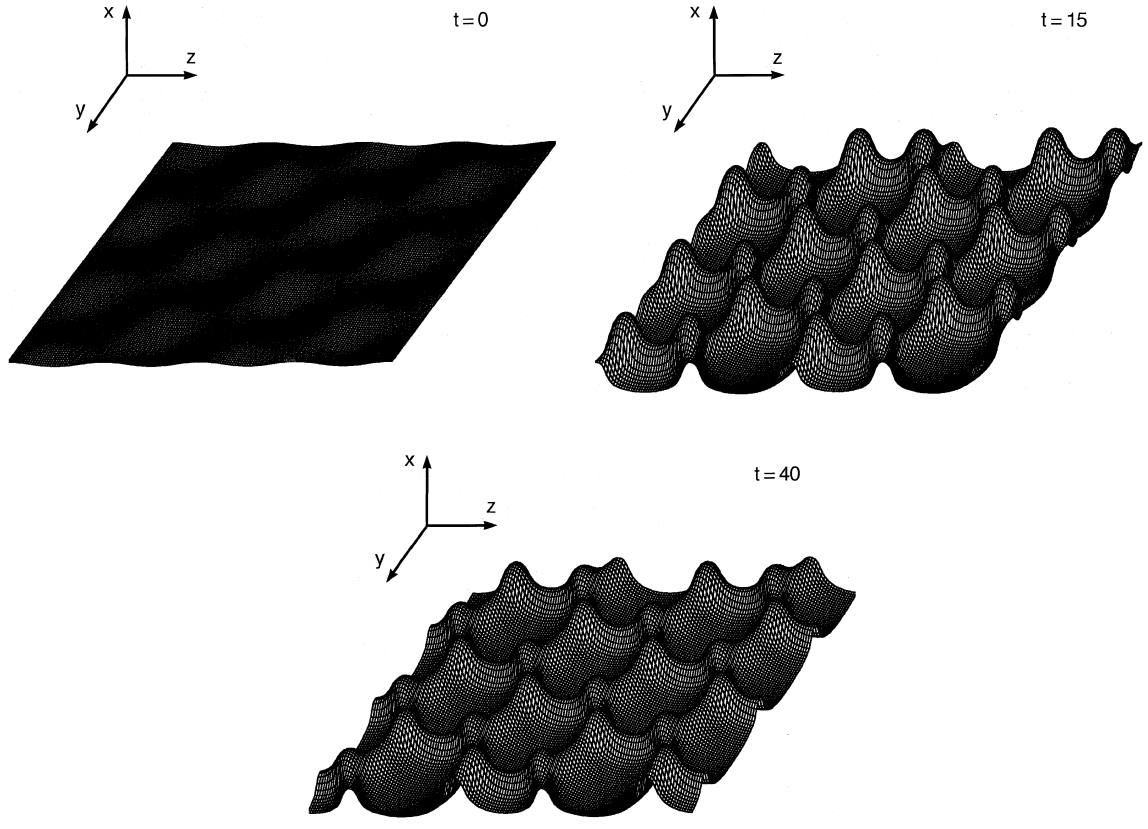

Fig. 2. Flame fronts for Le = 0.5, $A_0 = 1 \times 10^{-2}$, $\lambda_y = 0.166$, $\lambda_z = 0.288$ ($t = 0$, 15, and 40).

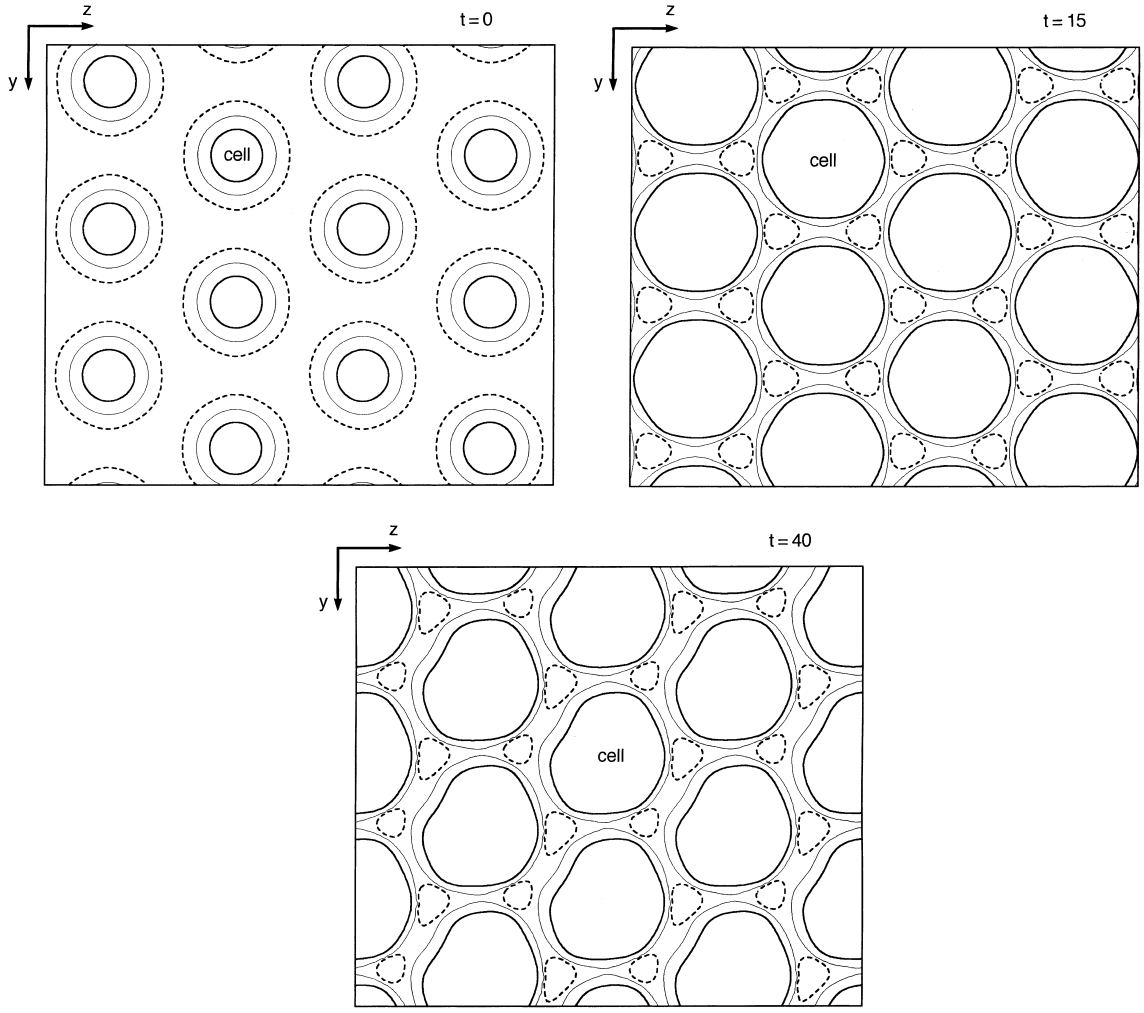

Fig. 3. Distributions of cells in the yz-plane for Le = 0.5, $A_0 = 1 \times 10^{-2}$, $\lambda_y = 0.166$, $\lambda_z = 0.288$; solid, hair, and broken lines denote contours of the flame front at $x = 0.587$, 0.593, and 0.599 ($t = 0$), $x = 0.551$, 0.591, and 0.630 ($t = 15$), $x = 0.441$, 0.475, and 0.509 ($t = 40$).

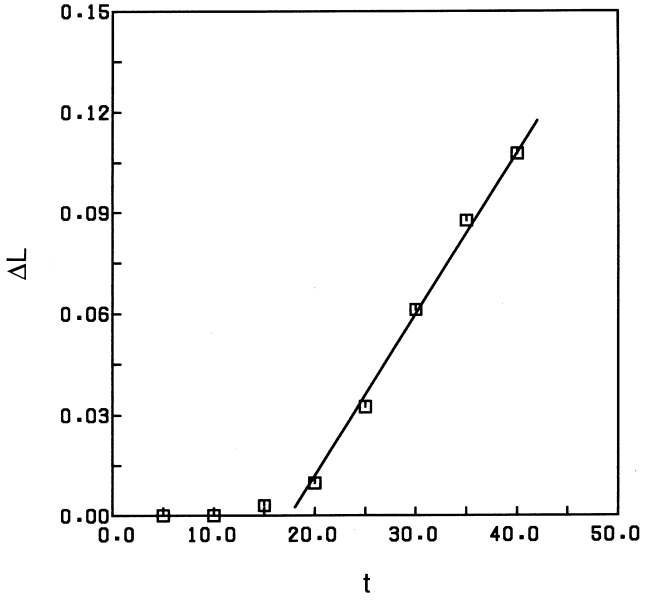

Fig. 4. Moved distance of the cell in the yz-plane for Le = 0.5 ($t = 5$–40).

$\lambda_z = 0.436$. The disturbance is evolved, and the cellular flame is formed. The cell moves slowly to the right-bottom, and its velocity is 0.17×10^{-3} ($= 0.07 S_u$) which is considerably large compared with that of the two-dimensional flame ($= 0.03 S_u$). When we apply the diffusive-thermal model to the flames used in the present study, we obtain $Le_c = 0.767$ since the activation energy is 70 and the adiabatic flame temperature is 7.0 (Sivashinsky, 1983). In the calculations based on the diffusive-thermal model, the lateral movement of cells appears at $Le < Le_c$. In the present calculation, on the other hand, laterally moving cells appear not only at $Le < Le_c$ but also at $Le_c < Le < 1$. This difference is due to the compressibility of gases.

Finally, we set Le = 1.0 to study the hydrodynamic effect on the lateral movement of cellular flames. The disturbance ($A_0 = 2 \times 10^{-2}$, $\lambda_y = 0.494$, $\lambda_z = 0.855$) superimposed on the plane flame is evolved, and the cellular flame is formed (Figs. 6 and 7). However, the location of cells in the yz-plane is immovable, which is dissimilar to $Le < 1$ flames. This result indicates that the lateral movement of cells is not generated only by the hydrodynamic effect. Thus, we know that the diffusive-thermal effect has an essential role in the lateral movement. When we set the inlet-flow velocity to the flame velocity of the cellular flame, we obtain the stationary flame. At $Le < 1$, on the other hand, we do not obtain the stationary cellular flame since cells move laterally.

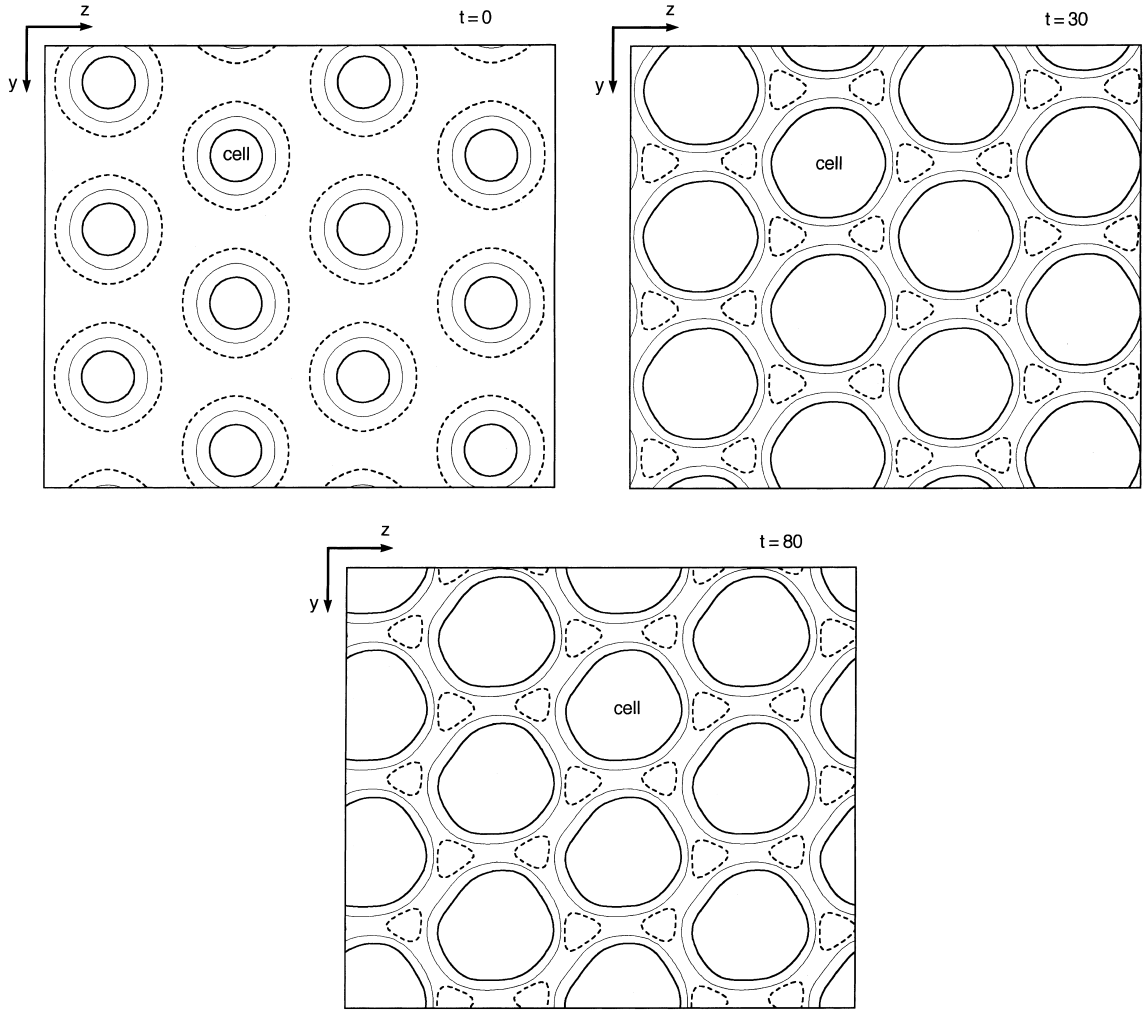

Fig. 5. Distributions of cells in the yz-plane for Le = 0.6, $A_0 = 1 \times 10^{-2}$, $\lambda_y = 0.185$, $\lambda_z = 0.320$; solid, hair, and broken lines denote contours of the flame front at $x = 0.587$, 0.593, and 0.599 ($t = 0$), $x = 0.525$, 0.550, and 0.575 ($t = 30$), $x = 0.374$, 0.399, and 0.423 ($t = 80$).

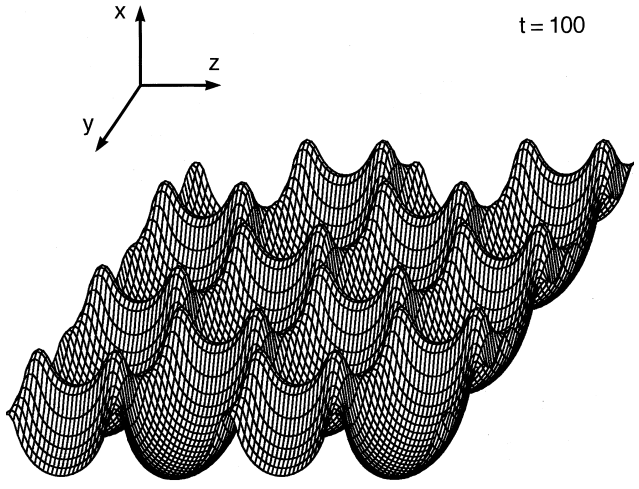

Fig. 6. Flame fronts for Le = 1.0, $A_0 = 2 \times 10^{-2}$, $\lambda_y = 0.494$, $\lambda_z = 0.855$ ($t = 100$).

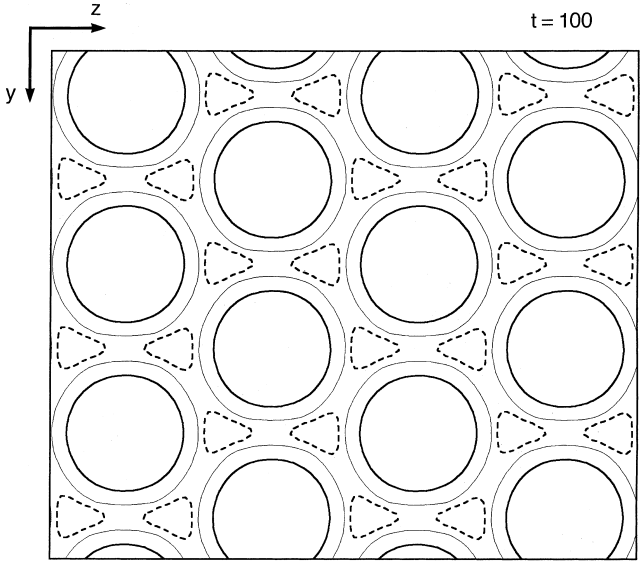

Fig. 7. Distributions of cells in the yz-plane for Le = 1.0, $A_0 = 2 \times 10^{-2}$, $\lambda_y = 0.494$, $\lambda_z = 0.855$; solid, hair, and broken lines denote contours of the flame front at $x = 0.520$, 0.584, and 0.647 ($t = 100$).

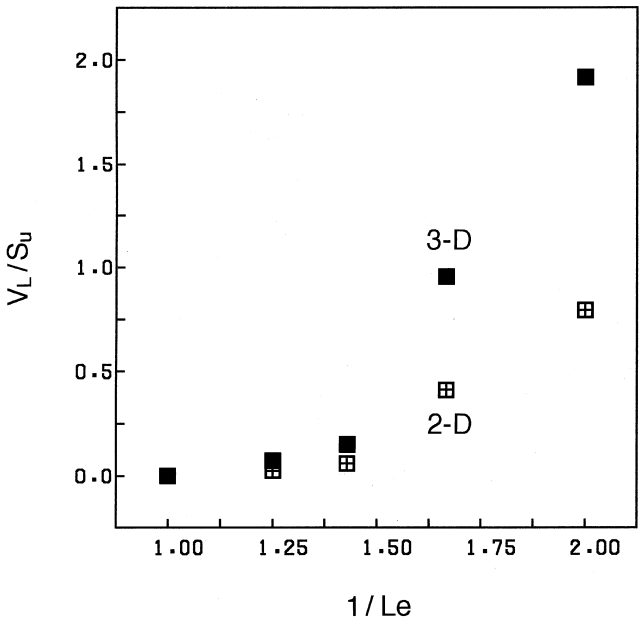

Fig. 8. Laterally moving velocities of the cell depending on the Lewis number for two- and three-dimensional flames.

The laterally moving velocities of the cell, which are normalized by the burning velocity, depending on the Lewis number for two- and three-dimensional flames are shown in Fig. 8. With a decrease in the Lewis number, the laterally moving velocity increases, since the instability level due mainly to the diffusive-thermal effect increases. Moreover, the laterally moving velocity of the three-dimensional cellular flame is much larger than that of the two-dimensional cellular flame.

When the Lewis number is lower than unity, the cellular flame moves laterally. When the Lewis number is unity, on the other hand, the cell position in the yz-plane is fixed. To study the mechanism of the lateral movement of cells, we illustrate the temperature distributions at the center of the cell for $Le = 0.5$, 0.6, and 1.0 in Fig. 9. Since the flame front at the cell center is convex toward the unburned gas, the local temperature of $Le < 1$ flames is raised owing to the diffusive-thermal effect. Thus, the maximum temperatures of $Le = 0.5$ and 0.6 flames are higher than the adiabatic flame temperature ($T_f = 7.0$). The temperature has an overshoot at the convex flame front, which is not observed in the $Le = 1.0$ flame. The physical phenomena associated with the overshoot are generally unstable. Therefore, the overshoot of temperature causes a breaking of the reflection symmetry of cells, and then the lateral movement of cells appears.

As the Lewis number decreases, the increment of local temperature at the convex flame front increases. Thus, the laterally moving velocity of the cell increases. Moreover, the increment of local temperature is great compared with that of the two-dimensional cellular flames. This is due to the difference in the disposition of cells between two- and three-dimensional flames. Therefore, the laterally moving velocity of the three-dimensional cellular flame is much larger.

5. Concluding remarks

We have calculated the three-dimensional unsteady reactive flow to investigate the lateral movement of cellular flames at low Lewis numbers. When only the hydrodynamic effect has an influence on the flame instability, the stationary cellular flame is formed. When the diffusive-thermal and hydrodynamic effects have an influence, on the other hand, the laterally moving cellular flame is formed not only at $Le < Le_c$ but also at $Le_c < Le < 1$. With a decrease in the Lewis number, the laterally moving velocity of the cell increases, which is due to the increase in the instability level. The laterally moving velocity of the three-dimensional cellular flame is much larger than that of the two-dimensional cellular flame. Because, the increment of local temperature at the convex flame front in the three-dimensional flame is great compared with that in the two-dimensional flame, which is due to the difference in the disposition of cells.

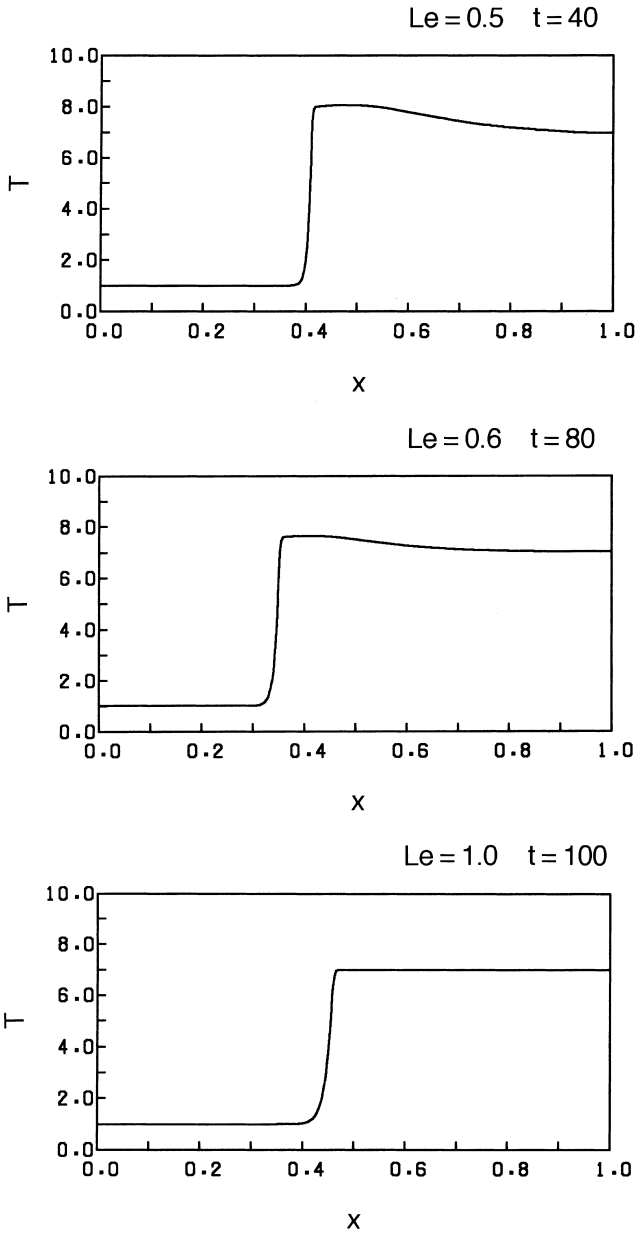

Fig. 9. Temperature distributions at the center of the cell for $Le = 0.5$ ($t = 40$), 0.6 ($t = 80$), and 1.0 ($t = 100$).

References

Barenblatt, G.I., Zeldovich, Y.B., Istratov, A.G., 1962. On diffusive-thermal stability of a laminar flame. J. Appl. Mech. Tech. Phys. 4, 21–26.

Bayliss, A., Matkowsky, B.J., 1992. Nonlinear dynamics of cellular flames. SIAM J. Appl. Math. 52, 396–415.

Bychkov, V.V., Golberg, S.M., Liberman, M.A., Eriksson, L.E., 1996. Propagation of curved stationary flames in tubes. Phys. Rev. E 54, 3713–3724.

Christopherson, D.G., 1940. Note on the vibration of membranes. Quart. J. Math. 11, 63–65.

Clavin, P., 1985. Dynamic behavior of premixed flame fronts in laminar and turbulent flows. Prog. Energy Combust. Sci. 11, 1–59.

Darrieus, G., 1938. Propagation d'un front de flamme. Unpublished works presented at La Technique Moderne.

Daumont, I., Kassner, K., Misbah, C., Valance, A., 1997. Cellular self-propulsion of two-dimensional dissipative structures and spatial-period tripling Hopf bifurcation. Phys. Rev. E 55, 6902–6906.

Denet, B., 1993. On non-linear instabilities of cellular premixed flames. Combust. Sci. Technol. 92, 123–144.

Denet, B., Bonino, J.L., 1994. Laminar premixed flame dynamics: A comparison of model and complete equations. Combust. Sci. Technol. 99, 235–252.

Denet, B., Haldenwang, P., 1992. Numerical study of thermal-diffusive instability of premixed flames. Combust. Sci. Technol. 86, 199–221.

Denet, B., Haldenwang, P., 1995. A numerical study of premixed flames Darrieus-Landau instability. Combust. Sci. Technol. 104, 143–167.

Gololobov, I.M., Granovskii, E.A., Gostintsev, Y.A., 1981. Two combustion modes at the limit of luminous flame propagation. Explos. Shock Waves 17, 22–26.

Gorman, M., el-Hamdi, M., Robbins, K.A., 1994. Experimental observation of ordered states of cellular flames. Combust. Sci. Technol. 98, 37–45.

Hyman, J.M., Nicolaenko, B., 1986. The Kuramoto-Sivashinsky equation: A bridge between PDE's and dynamical systems. Physica D 18, 113–126.

Joulin, G., Mitani, T., 1981. Linear stability analysis of two-reactant flames. Combust. Flame. 40, 235–246.

Kadowaki, S., 1995. Numerical analysis on instability of cylindrical flames. Combust. Sci. Technol. 107, 181–193.

Kadowaki, S., 1996. Numerical study on the instability of premixed plane flames in the three-dimensional field. Int. J. Heat Fluid Flow 17, 557–566.

Kadowaki, S., 1997. Numerical study on lateral movements of cellular flames. Phys. Rev. E 56, 2966–2971.

Landau, L.D., 1944. On the theory of slow combustion. Acta Phys. 19, 77–85.

Law, C.K., 1988. Dynamics of stretched flames. Twenty-second Symposium (International) on Combustion, The Combustion Institute, Pittsburgh, pp. 1381-1402.

MacCormack, R.W., Baldwin, B.S., 1975. A numerical method for solving the Navier–Stokes equations with application to shock-boundary layer interactions. AIAA paper, 75-1.

Markstein, G.H., 1964. Nonsteady Flame Propagation. Pergamon, Oxford pp. 75–105.

Margolis, S.B., Matkowsky, B.J., 1983. Nonlinear stability and bifurcation in the transition from laminar to turbulent flame propagation. Combust. Sci. Technol. 34, 45–77.

Michelson, D.M., Sivashinsky, G.I., 1982. Thermal-expansion induced cellular flames. Combust. Flame 48, 211–217.

Patnaik, G., Kailasanath, K., 1994. Numerical simulations of burner-stabilized hydrogen-air flames in microgravity. Combust. Flame 99, 247–253.

Pearlman, H.G., Ronney, P.D., 1994. Near-limit behavior of high-Lewis number premixed flames in tubes at normal and low gravity. Phys. Fluids 6, 4009–4018.

Sabathier, F., Boyer, L., Clavin, P., 1981. Experimental study of a weak turbulent premixed flame. Prog. Astronaut. Aeronaut. 76, 246–258.

Searby, G., Quinard, J., 1990. Direct and indirect measurements of Markstein numbers of premixed flames. Combust. Flame 82, 298–311.

Shtilman, L., Sivashinsky, G.I., 1990. On the hexagonal structure of cellular flames. Can. J. Phys. 68, 768–771.

Sivashinsky, G.I., 1977. Diffusional-thermal theory of cellular flames. Combust. Sci. Technol. 15, 137–146.

Sivashinsky, G.I., 1983. Instabilities, pattern formation, and turbulence in flames. Ann. Rev. Fluid Mech. 15, 179–199.

Williams, F.A., 1985. Combustion Theory, 2nd ed. Ch. 9. Addison-Wesley, Reading, MA.